



**HAL**  
open science

## An insight into the unloading/reloading loops on the compression curve of natural stiff clays

Yu-Jun Cui, Xuan-Phu Nguyen, Anh Minh A.M. Tang, Xiang-Ling Li

► **To cite this version:**

Yu-Jun Cui, Xuan-Phu Nguyen, Anh Minh A.M. Tang, Xiang-Ling Li. An insight into the unloading/reloading loops on the compression curve of natural stiff clays. *Applied Clay Science*, 2013, 83-84, pp.343-348. hal-00926893

**HAL Id: hal-00926893**

**<https://enpc.hal.science/hal-00926893>**

Submitted on 25 Apr 2018

**HAL** is a multi-disciplinary open access archive for the deposit and dissemination of scientific research documents, whether they are published or not. The documents may come from teaching and research institutions in France or abroad, or from public or private research centers.

L'archive ouverte pluridisciplinaire **HAL**, est destinée au dépôt et à la diffusion de documents scientifiques de niveau recherche, publiés ou non, émanant des établissements d'enseignement et de recherche français ou étrangers, des laboratoires publics ou privés.



24 **Abstract**

25 Oedometer tests were carried out with loading/unloading/reloading on natural saturated  
26 Ypresian clay taken from several depths. Common unloading/reloading loops were identified.  
27 Further examination of the unloading or reloading curves shows that each path can be  
28 satisfactorily considered as bi-linear with a small and a larger slopes separated by a threshold  
29 vertical stress. This threshold stress can be considered as the swelling pressure corresponding  
30 to the void ratio just before the unloading or reloading. Indeed, upon unloading, when the  
31 applied stress is higher than the threshold stress or swelling pressure, the mechanical effect is  
32 dominant and only small mechanical rebound is observed, corresponding to a small  
33 microstructure change; by contrast, when the applied stress is lower than the swelling  
34 pressure, physico-chemical effect becomes prevailing, and soil swelling occurs with a larger  
35 microstructure change. Upon reloading, when the applied stress is lower than the swelling  
36 pressure, the microstructure is not significantly affected thanks to the contribution of the  
37 physico-chemical repulsive force, leading to a small volume change; on the contrary, beyond  
38 the swelling pressure, the mechanical effect becomes dominant giving rise to larger volume  
39 change corresponding to the microstructure collapse. Like unsaturated expansive soils, it is  
40 found that there is a good relationship between the swelling pressure (threshold stress) and the  
41 void ratio just before the unloading or reloading. This is confirmed by the results from the  
42 data reported in the literature on Boom and London clays. It can be then deduced that the  
43 unloading/reloading loop is rather due to the competition between the mechanical and  
44 physico-chemical effects on the microstructure changes than the viscosity effect as commonly  
45 admitted.

46 **Keywords:** clays; unloading/reloading loops; oedometer tests; mechanical effect, physico-  
47 chemical effect; swelling pressure.

48

## 49 **Introduction**

50 It is well known that the soil compression curves show unloading/reloading loops. These  
51 loops have been commonly explained by the soil viscosity effect: clayey soils have larger  
52 loops because of their relatively higher viscosity, and sandy soils have narrow loops because  
53 of their low viscosity, silty soils being in between. Indeed, Coop & Lee (1993) performed  
54 compression tests on the Ham River sand and Dogs bay sand, and the results from  
55 unloading/reloading paths show a negligible hysteresis without any marked loops. However,  
56 the unloading/reloading loop is quite clear for silty soils (see Nasreddine 2004 for instance ),  
57 and becomes much more marked for clayey soils (Holtz et al. 1986), bentonite (Borgesson et  
58 al. 1996), bentonite/sand mixtures (Tong & Yin 2011), kaolin/bentonite mixture (Di Maio et  
59 al. 2004), and claystone (Mohajerani et al. 2011). When investigating the compressibility of a  
60 soil, these loops are often ignored and an average slope is usually considered in the  
61 calculation of soil volume change. Obviously, this practice is relatively easy for sandy soils  
62 and silty soils, but difficult for clayey soils and even impossible for expansive soils.

63 From a fundamental point of view, explaining the unloading/reloading loops by viscosity  
64 effect seems too simplistic and unclear. Further study on the corresponding mechanisms is  
65 needed. But to the authors' knowledge, there is up to now no plausible mechanisms developed  
66 allowing correctly explaining the soil volume change behaviour under unloading/reloading. In  
67 this study, this aspect was investigated by performing oedometer tests with several  
68 unloading/reloading cycles on natural Ypresian stiff clays. The results were analysed based on  
69 the competition between the mechanical effect and physico-chemical effect occurred during  
70 unloading or reloading. A new mechanism related to the soil swelling pressure was proposed.  
71 This mechanism was verified by the results from the oedometer tests on other natural stiff  
72 clays such as Boom clay and London clay.

## 73 **Materials and methods**

74 The materials studied are cores sampled from Ypresian formation at four different depths,  
75 namely YP43 from 330.14 m - 330.23 m depth, YP64 from 351.20 m - 351.29 m depth, YP  
76 73 from 361.30 m- 361.34 m depth, and YP95 from 382.35 m - 382.44 m depth. Their clay  
77 mineralogy and physical properties are shown in Table 1 and Table 2, respectively. The four  
78 depths have comparable clays fraction (between 48 and 59%) as well as similar smectite  
79 content (between 26 and 34%), suggesting similar physical properties in terms of plasticity.  
80 However, the values of plasticity index  $I_p$  and methylene blue VBS (see Table 2) shows a  
81 much lower plasticity of YP43 as compared to the three other depths. YP43 has also the  
82 lowest liquid limit ( $w_L = 75$ ) and the highest carbonates content  $\text{CaCO}_3$  (10.16%), its other  
83 parameters (specific gravity  $G_s$ , plastic limit  $w_p$ , initial water content  $w_0$ , initial void ratio  $e_0$ )  
84 being similar to that of other depths. It is possible that the high carbonates content of YP43  
85 gives rise a lower level of plasticity as indicated by the values of  $I_p$  and VBS in Table 2.  
86 Further study is needed to clarify this point.

87 Oedometer tests were performed on soil samples of 50-mm diameter and 20-mm height by  
88 hand-trimming from cores that have 1000-mm length and 100-mm diameter. After installing  
89 soil sample in the oedometer cell, step loading up to the in situ vertical effective stress (up to  
90 point A in Figure 1a) was carried out without contact with water in order to avoid any  
91 swelling which would affect the initial soil microstructure (Delage et al., 2007; Cui et al.  
92 2009, Deng et al., 2011a, 2011b, 2011c). Note that the in-situ vertical effective stresses ( $\sigma'_{v0}$ )  
93 were estimated by taking an average mass density of overburden soils equal to  $1.9 \text{ Mg/m}^3$   
94 (Van Marcke & Laenen, 2005) with an underground water level assumed to be at the ground  
95 surface. For a reason of convenience,  $\sigma'_{v0}$  were rounded to 3.2 MPa for all the four depths.

96 The degree of saturation at point A, calculated using the initial degree of saturation (see  $S_{r0}$  in  
97 Table 2) and the volume change recorded, was found to be 100% for all samples tested.

98 Under  $\sigma'_{v0}$ , the bottom porous stone and the drainage tubes were saturated with the in-situ  
99 synthetic water that has the same chemical composition as the field water (A-B). Afterwards,  
100 step unloading to 0.125 MPa (B-C), reloading up to 16 MPa (C-D), unloading again to 0.125  
101 MPa (D-E), reloading up to 32 MPa (E-F) and finally unloading to 0.125 MPa (F-G) were  
102 conducted. The stabilization of volume change was considered as achieved when the vertical  
103 strain rate is lower than  $5 \times 10^{-4}/8$  h (AFNOR, 1995, 2005).

104

## 105 **Test results**

106 Figure 1 shows the compression curve for the four depths. For YP43 (Figure 1a), YP64  
107 (Figure 1b) and YP73 (Figure 1c), two full unloading/reloading cycles and one extra single  
108 unloading were applied, while for YP95 (Figure 1d), only one full cycle and one extra single  
109 unloading were applied. Figure 1a shows that the application of the in-situ vertical stress  
110 (3.2 MPa) led the soil sample to point A. When saturating the bottom porous stone and the  
111 drainage tubes, a negligible volume change (A to B) was observed, confirming that the  
112 sample was fully saturated. Upon unloading from B to C, a nearly bi-linear curve was  
113 observed: when the stress was higher than a threshold stress  $\sigma_{s1}$  the slope was small, and  
114 when the stress was lower than  $\sigma_{s1}$  the slope is significantly larger. Upon reloading from C to  
115 D, a tri-linear curve was identified. Below the stress at point B, a nearly bi-linear curve was  
116 again observed, with a small slope below a threshold stress  $\sigma_{s4}$  and a larger slope beyond  $\sigma_{s4}$ .  
117 Further loading beyond point B gave rise to a larger slope, certainly related to the plastic  
118 volume changes. Examination of the unloading/reloading curve B-C-B shows a hysteretic

119 loop. The same phenomenon can be observed when unloading the sample from D to E and  
120 reloading the sample from E to F: there is a nearly bi-linear curve from D to E with a small  
121 slope beyond a threshold stress  $\sigma_{s2}$  and larger slope below  $\sigma_{s2}$ , there is also a nearly bi-linear  
122 curve from E to D with a threshold stress  $\sigma_{s3}$ , and when the stress is beyond point D, the slope  
123 is increased because of the plastic volume change. The unloading from F to G confirmed the  
124 bi-linearity of the curve with a threshold stress  $\sigma_{s3}$ . Comparison of the unloading slopes shows  
125 that both the small slope and large slope were increasing with the maximum stress applied  
126 prior to unloading.

127 The same observation can be made on the results from the tests on the other three depths  
128 (YP64 – Figure 1b, YP73 – Figure 1c and YP95 – Figure 1d). There are also more or less well  
129 defined bi-linear curves for both unloading and reloading paths with threshold stresses.

130 It must be mentioned that the bi-linearity observed in this study should be considered as a  
131 particular case because for most soils non-linear curves are often observed. It is likely that  
132 there is relatively well defined bi-linearity for natural stiff clays like the studied natural  
133 Ypresian clay. Basically, the shape of the curves depends on both the soil nature and soil  
134 microstructure.

135 To further analyse the results, in Figure 2, the values of threshold stress in Figure 1 for each  
136 depth are presented as a function of the void ratio just before each unloading or reloading ( $\sigma_{s1}$   
137 with  $e_{i1}$ ;  $\sigma_{s2}$  with  $e_{i2}$ ;  $\sigma_{s3}$  with  $e_{i3}$ ;  $\sigma_{s4}$  with  $e_{i4}$ ;  $\sigma_{s5}$  with  $e_{i5}$ ). A good linear relationship is  
138 obtained in a semi-logarithmic plane for all the four depths. In order to verify this  
139 observation, some results from oedometer tests on other stiff clays from the literature are  
140 collected, and shown in Figure 3 together with the results of Ypresian clay. It is observed that  
141 the variations of swelling pressure with the initial void ratio before unloading or reloading for  
142 Boom clay from Essen taken at different depths (Ess 75, Ess 83, Ess 96, Ess 104, Ess112) and

143 for Boom clay from Mol (Deng et al. 2011a, Horseman et al. 1987) show also good linear  
144 functions. Obviously, the relationship between  $\sigma_s$  and  $e_i$  is soil nature dependent: the slope is  
145 different for different soils.

146 Figure 4 shows the results obtained on the basis of the data reported by Gasparre and Coop  
147 (2008) on London clay at Heathrow Airport Terminal 5. It involves six samples from  
148 different depths: 7 m (C7), 10 m (B10), 25 m (B25), 28 m (B28), 36 m (A36) and 51 m  
149 (A51). Again, a good linear relationship is observed for all samples with unloading/reloading.

## 150 **Interpretation and discussion**

151 Delage and Lefebvre (1984) showed that when compressing a clayey soil in oedometer,  
152 macro-pore collapse occurs first during loading path under stresses higher than the  
153 preconsolidation pressure or yield stress of soil, leading to irrecoverable volume changes; this  
154 process results in microstructure changes characterized by more and more orientated particles.  
155 As Le et al. (2011) indicated with a more orientated microstructure the physico-chemical  
156 interaction between clay particles and adsorbed water is enhanced. Indeed, Olson and Mesri  
157 (1970) pointed out that the competition between the mechanical effect and physico-chemical  
158 effect on soil volume change behaviour depends strongly on the particles geometric  
159 arrangement defined by the contact angle between particles: the mechanical effect is more  
160 pronounced when the contact angle is large, and on the contrary, the physico-chemical effect  
161 becomes dominant when the particles are more parallel with a small contact angle. Thereby,  
162 upon mechanical loading in oedometer the contact angle is decreasing, leading to increase of  
163 the physico-chemical effect.

164 Basically, the increase of physico-chemical effect due to loading can be well evidenced  
165 during unloading: the more orientated particles undergo higher repulsion forces and thus show  
166 more significant swell: the unloading curve could have a much greater slope than the initial

167 loading slope before the preconsolidation pressure is reached, and the void ratio after full  
168 unloading could even be higher than the initial void ratio. Examination of the unloading  
169 slopes in Figure 1 confirms this reasoning: the unloading slope is indeed increasing with  
170 increasing yield stress.

171 The description above shows that when unloading from the previous maximum stress  
172 (commonly termed as yield stress), the compression behaviour is mainly governed by the  
173 competition between the physico-chemical effect and mechanical effect. When the external  
174 stress is higher than the repulsive force related to the soil particles-water interaction (physico-  
175 chemical effect), low swelling volume change occurs; otherwise higher swelling volume  
176 change can be expected. Similarly, upon reloading, when the external stress is lower than the  
177 repulsive force related to the physico-chemical effect, this external stress is balanced by the  
178 repulsive force, leading to a small volume decrease; on the contrary, when the external stress  
179 becomes higher, the mechanical effect becomes dominant giving rise to larger volume  
180 decrease. This conceptual description implies that it is possible to determine some  
181 characteristic stress that separate the zone with prevailing physico-chemical effect from the  
182 zone with prevailing mechanical effect. It is indeed what is observed in Figure 1 with the  
183 threshold stress. Upon unloading, when the vertical stress is higher than the threshold stress  
184  $\sigma_s$ , the volume change is characterized by the mechanical rebound; however, in the lower  
185 stress range the volume change is characterized by the physico-chemical swelling.

186 Furthermore, if we admit that the physico-chemical effect mentioned above corresponds to  
187 the matric suction as we do commonly for expansive soils (saturated or unsaturated), the  
188 threshold stress identified should correspond to the swelling pressure. Indeed, the swelling  
189 pressure of a soil is commonly defined as the stress under which no volume change occurs  
190 upon wetting. According to this definition, swelling takes place when wetting a soil under a

191 stress lower than the swelling pressure; on the contrary, collapse takes place when wetting the  
192 soil under a stress higher than the swelling pressure. Thus, the swelling pressure can  
193 experimentally be determined by loading the soil samples in oedometer to different vertical  
194 stress  $\sigma_v'$  and then wetting them (see Figure 5a). Various other methods can be used for this  
195 purpose (see Figure 5b). The “constant-volume” method (path OA) is based on the use of a  
196 relatively rigid cell with total pressure measurement (Tang et al., 2011, Wang et al. 2012).  
197 The value of pressure after stabilisation is the swelling pressure of soil. For the “zero-swell”  
198 method (path OBB’) the equipment employed is a conventional oedometer (Basma et al.,  
199 1995; Nagaraj et al., 2009). Firstly, a low initial load (0.1 MPa for example) is applied on the  
200 specimen prior to water flooding. As the specimen wets up it attempts to swell. When the  
201 swell exceed a certain value (0.1% for example), additional pressure is added in small  
202 increment to bring the volume of soil specimen back to its initial value (Basma et al., 1995;  
203 Attom et al., 2001). This operation is repeated until the specimen ceases to swell. The  
204 swelling pressure is defined as the stress under which no more swelling occurs. The “swell-  
205 consolidation” method (path OCC’) consists of re-saturating the soil under a low pressure (0.1  
206 MPa for example). After swell completion, standard consolidation test is performed. The  
207 pressure required to bring the soil specimen back to its original void ratio is defined as the  
208 swelling pressure (Basma et al., 1995; Agus, 2005).

209 The small mechanical rebound upon unloading implies an insignificant microstructure  
210 change, i.e., the microstructure pattern remains rather orientated with dominated face-to-face  
211 particle contacts (see Figure 6). When the external stress is lower than the threshold stress or  
212 swelling pressure  $\sigma_s$ , the prevailing physico-chemical effect leads to a significant  
213 microstructure change characterized by formation of more and more face-to-edge particle  
214 contacts. This microstructure change corresponds to a larger soil swelling. From this  
215 description, the threshold stress or swelling pressure  $\sigma_s$  separates the zone with insignificant

216 microstructure change from the zone with significant microstructure change. The increase of  
217 this swelling pressure with loading ( $\sigma_{s1} < \sigma_{s2} < \sigma_{s3}$ ) observed in Figure 1 is also consistent  
218 with the common results on unsaturated expansive soils: a higher stress causes lower void  
219 ratio or higher density, increasing the swelling pressure (Villar et al., 2008; Siemens et al.,  
220 2009; Wang et al., 2012).

221 The reasoning above applies also for the reloading path. When the external stress is lower  
222 than the swelling pressure, the matric suction related to the physico-chemical effect is high  
223 enough to balance the effect of external stress, and the current microstructure changes  
224 insignificantly (with the face-to-edge particles preserved). As a result, the slope of the  
225 compression curve is small. By contrast, when the external stress is higher than the swelling  
226 pressure, the mechanical effete becomes dominant and larger volume change occurs by  
227 collapse of large-pores (the particles arrangement tends towards face-to-face type), leading to  
228 a larger slope of the compression curve. This is also consistent with the swelling pressure  
229 definition shown in Figure 5.

230 It should be mentioned that the model used above for microstructure changes during  
231 unloading/reloading is totally conceptual. It should be confirmed by experimental evidences  
232 provided in further studies implying appropriate techniques. Theoretically, the more plastic  
233 the soil is (high smectite content, high plasticity index  $I_p$ , large methylene blue value, etc.),  
234 the more microstructure changes from face-to-face pattern to face-to-edge pattern can be  
235 expected.

236 Figures 2-4 show that there is a linear relationship between swelling pressure and the void  
237 ratio before unloading or reloading in a semi-logarithmic scale for natural stiff clays as  
238 Ypresian clay, Boom clay and London clay, although this relationship is soil nature  
239 dependent. This is consistent with the results from the tests on unsaturated expansive soils,

240 thereby bring another evidence for the identified threshold stress as swelling pressure. Note  
241 that for other soils there is not necessarily bi-linear unloading/reloading curves, thus, difficult  
242 to determine the relationship between the swelling pressure and void ratio before unloading or  
243 reloading. However, it is believed that the conceptual model developed in this study would be  
244 still applicable.

## 245 **Conclusion**

246 Oedometer tests were carried out with loading/unloading/reloading on saturated natural  
247 Ypresian clay from different depths. The unloading/reloading loops of compression curves of  
248 Ypresian clay have been explained by the competition between the mechanical and physico-  
249 chemical effects. Upon unloading, when the applied stress is higher than the swelling  
250 pressure, the mechanical effect is dominant and only small mechanical rebound is observed;  
251 by contrast, when the applied stress is lower than the swelling pressure, physico-chemical  
252 effect becomes dominant, giving rise to soil swelling with a larger slope. Upon reloading,  
253 when the applied stress is lower than the swelling pressure, the microstructure is more or less  
254 preserved thank to the contribution of the matric suction, leading to a small volume change;  
255 on the contrary when the applied stress is higher than the swelling pressure, the mechanical  
256 effect prevails and larger volume change occurs by collapse of large-pores. The good linear  
257 relationship between the swelling pressure and the void ratio just before unloading or  
258 reloading confirms this interpretation. Further examination of Boom clay from both Essen and  
259 Mol sites as well as London clay brings further confirmation to this concept. It can be then  
260 concluded that the unloading/reloading loop is rather due to the competition between the  
261 mechanical and physico-chemical effects than the viscosity effect as commonly admitted.  
262 Note however that this interpretation was done only based on the oedometer tests on natural

263 stiff clays. Further studies are needed to make more clarification, especially in terms of  
264 microstructure investigation.

265

## 266 **References**

- 267 AFNOR, 1995. Sols : reconnaissance et essais: essai de gonflement à l'oedomètre,  
268 détermination des déformations par chargement de plusieurs éprouvettes. XP P 94-091.
- 269 AFNOR, 2005. Geotechnical investigating and testing, Laboratory testing of soils, Part 5:  
270 Incremental loading Oedometer test. XP CEN ISO/TS 17892-5.
- 271 Agus, S., 2005. An Experimental study on hydro-mechanical characteristics of compacted  
272 bentonite-sand mixtures. PhD thesis. Weimar.
- 273 Attom, M., Abu-Zreig, M. & Obaidat, M., 2001. Changes in clay swelling and shear strength  
274 properties with different sample preparation techniques. Geotechnical Testing Journal,  
275 ASTM, 24, 157-163.
- 276 Basma,A.A., Al-Homoud, A.S., Husein, A., 1995. Laboratory assessment of swelling  
277 pressure of expansive soils. Applied Clay Science, 9(5), 355–368.
- 278 Borgesson, L., Karnland, O., Johannesson, L. E., 1996. Modelling of the physical behaviour  
279 of clay barriers close to water saturation. Engineering Geology, 41, 127-144.
- 280 Coop, M. R., Lee, I. K., 1993. The behaviour of granular soils at elevated stresses. Proc.  
281 Wroth Memorial Symposium: Predictive soil mechanics, pp. 186 - 198.
- 282 Cui Y.J., Le T.T., Tang A.M., Delage P., Li X.L., 2009. Investigating the time dependent  
283 behaviour of Boom clay under thermo-mechanical loading. Géotechnique, 59 (4), 319-  
284 329.
- 285 Delage P., Lefebvre G., 1984. Study of the structure of a sensitive Champlain clay and of its  
286 evolution during consolidation. Canadian Geotechnical Journal, 21 (1), 21-35.

287 Delage P., Le T.T., Tang A.M., Cui Y.J., Li X.L., 2007. Suction and in-situ stresses of deep  
288 Boom clay samples. *Géotechnique*, 57(1), 239-244.

289 Deng Y. F., Tang A. M., Cui Y. J., Nguyen X. P., Li X. L., Wouters L., 2011a. Laboratory  
290 Hydro-mechanical Characterisation of Boom Clay at Essen and Mol. *Physics and*  
291 *Chemistry of the Earth*, 36 (17-18), 1878–1890.

292 Deng Y.F., Tang A.M., Cui Y.J., Li X.L., 2011b. A study on the hydraulic conductivity of  
293 Boom clay. *Canadian Geotechnical Journal*, 48, 1461-1470.

294 Deng Y. F., Cui Y. J., Tang A. M., Nguyen X. P., Li X. L., Van Geet M., 2011c. Investigating  
295 the pore-water chemistry effects on the volume change behaviour of Boom clay. *Physics*  
296 *and Chemistry of the Earth*, 36 (17-18), 1905–1912.

297 Di Maio, C., Santoli, L., Schiavone, P., 2004. Volume change behaviour of clays: the  
298 influence of mineral composition, pore fluid composition and stress state. *Mechanics of*  
299 *Materials*, 36, 435–451.

300 Gasparre, A., Coop, M. R., 2008. Quantification of the effects of structure on the compression  
301 of a stiff clay. *Canadian Geotechnical Journal*, 45(9), 1324-1334.

302 Holtz, R. D., Jamiolkowski, M. B., Lancellotta, R., 1986. Lessons from oedometer tests on  
303 high quality samples. *Journal of Geotechnical Engineering*, 112(8), 768-776.

304 Horseman, S.T., Winter M.G., Entwistle D.C., 1987. Geotechnical characterization of Boom  
305 clay in relation to the disposal of radioactive waste. Commission of the European  
306 Communities, EUR 10987, 87 p.

307 Le T.T., Cui Y.J., Munoz J.J., Delage P., Tang A.M., Li X., 2011. Studying the stress-suction  
308 coupling in soils using an oedometer equipped with a high capacity tensiometer. *Front.*  
309 *Archit. Civ. Eng.China*, 5(2), 160–170.

310 Mohajerani M., Delage P., Monfared M, Tang A.M., Sulem J., Gatmiri, B. 2011. Oedometer  
311 compression and swelling behaviour of the Callovo-Oxfordian argillite. *International*

312 Journal of Rock Mechanics and Mining Sciences, 48(4), 606 – 615.  
313 (doi:10.1016/j.ijrmms.2011.02.01)

314 Nagaraj, H. MOHAMMED Munnas, M. Sridharan,A., 2009. Critical Evaluation of  
315 Determining Swelling Pressure by Swell-Load Method and Constant Volume Method,  
316 Geotechnical Testing Journal, ASTM, 32, 305-314.

317 Nasreddine, K. 2004. Effet de la rotation des contraintes sur le comportement des sols  
318 argileux. PhD thesis, Ecole Nationale des Ponts et Chaussées, Paris.

319 Olson R. O., Mesri G., 1970. Mechanisms controlling compressibility of clays. Journal of Soil  
320 Mechanics and Foundation Division, Proceeding of the American Society of Civil  
321 Engineers. SM6, pp. 1863-1878

322 Siemens, G., Blatz, J.A., 2009. Evaluation of the influence of boundary confinement on the  
323 behaviour of unsaturated swelling clay soils. Canadian Geotechnical Journal, 46(3), 339–  
324 356.

325 Tang C. S., Tang A. M., Cui Y. J., Delage P., Sshroeder C., De Laure E., 2011. Investigating  
326 the Swelling Pressure of Compacted Crushed-Callovo-Oxfordian Argillite. Physics and  
327 Chemistry of the Earth, 36 (17-18), 1857–1866.

328 Tong, F., Yin, J. H., 2011. Nonlinear Creep and Swelling Behavior of Bentonite Mixed with  
329 Different Sand Contents Under Oedometric Condition. Marine Georesources &  
330 Geotechnology, 29(4), 346-363.

331 Vandenberghe N., 2011. Qualitative & quantitative mineralogical analyses on the Ypresian  
332 clay. Report of Applied Geology & Mineralogy Group of K. U. Leuven to NIRAS-  
333 ONDRAF.

334 Van Marcke Ph., Laenen B. 2005. The Ypresian clays as possible host rock for radioactive  
335 waste disposal: an evaluation. Report of Belgian agency for radioactive waste and  
336 enriched fissile materials, 149p.

- 337 Villar, M.V., Lloret, A., 2008. Influence of dry density and water content on the swelling of a  
338 compacted bentonite. *Applied Clay Science*, 39(1-2), 38–49.
- 339 Wang Q., Tang A.M., Cui Y.J., Delage P., Gatmiri B. 2012. Experimental study on the  
340 swelling behaviour of bentonite/claystone mixture. *Engineering Geology*, 124, 59-66.
- 341

342 **List of Tables**

343 Table 1. Mineralogy of Ypresian clay (Vandenberghe et al., 2011)

344 Table 2. Physical properties of Ypresian clay

345

346

347 **List of Figures**

348 Figure 1. Oedometer test with unloading/reloading on Ypresian clays

349 Figure 2. Swelling stress versus the void ratio just before unloading or reloading for Ypresian  
350 clays - Closed symbols are for unloading path, open symbols for loading path.

351 Figure 3. Swelling stress versus the void ratio just before unloading or reloading for Boom  
352 (from both Essen and Mol sites) and Ypresian clays. - Closed symbols are for unloading path,  
353 open symbols for loading path

354 Figure 4. Swelling stress versus the void ratio just before unloading or reloading for London  
355 clay. - Closed symbols are for unloading path, open symbols for loading path

356 Figure 5. Methods for swelling pressure determination. (a) loading-wetting method, (b)  
357 constant-volume, zero-swell and swell-consolidation methods

358 Figure 6. Representation of microstructure changes during unloading/reloading

359

360

361

362

363

364

**Table 1. Mineralogy of Ypresian clay (Vandenberghe et al., 2011)**

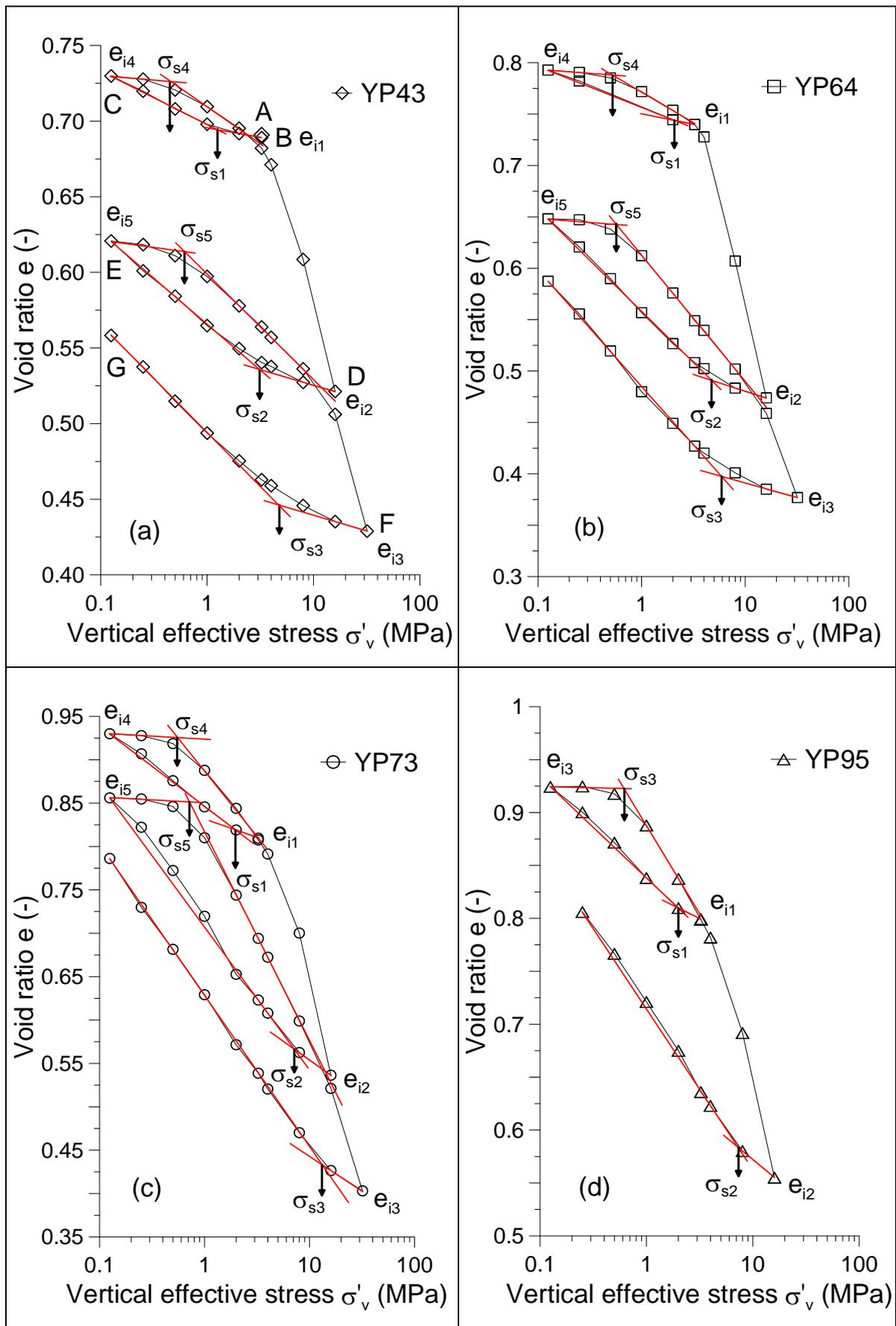
Mineral	YP43	YP64	YP73	YP95
Depth (m)	330.14-330.23	351.20-351.29	361.30-361.34	382.35-382.44
$\Sigma$ Clay (% wt)	<b>54</b>	<b>48</b>	<b>57</b>	<b>59</b>
Illite	5	4	5	6
Kaolinite	2	5	3	3
Smectite	32	26	33	34
Illite/Smectite	12	10	12	13
Chlorite/others	3	3	4	3
$\Sigma$ Non-clay (% wt)	<b>46</b>	<b>52</b>	<b>43</b>	<b>41</b>
Quartz	32	36	31	27
K-feldspar	6	7	6	7
Plagioclase	6	6	5	3
Others	2	3	1	4

365

366

**Table 2. Physical properties of Ypresian clay**

Soil	$G_s$ (-)	$w_L$ (-)	$w_P$ (-)	$I_P$ (-)	$w_0$ (%)	$e_0$ (-)	$S_{r0}$ (%)	VBS (g/100g)	CaCO <sub>3</sub> (%)
YP43	2.78	75	34	42	26	0.81	89	3.95	10.16
YP64	2.79	114	34	80	26	0.79	92	7.09	1.38
YP73	2.80	137	36	101	31	0.94	93	13.12	0.88
YP95	2.80	132	44	88	30	0.95	87	12.72	3.82

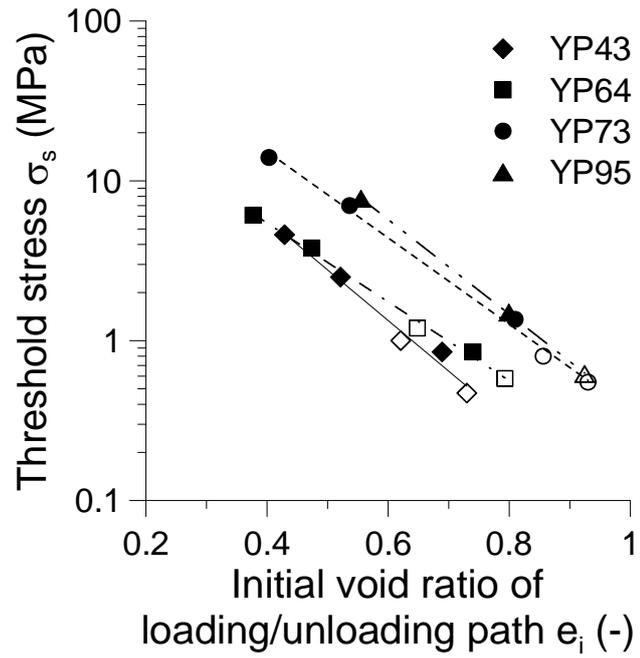


368

Figure 1. Oedometer test with unloading/reloading on Ypresian clays

369

370

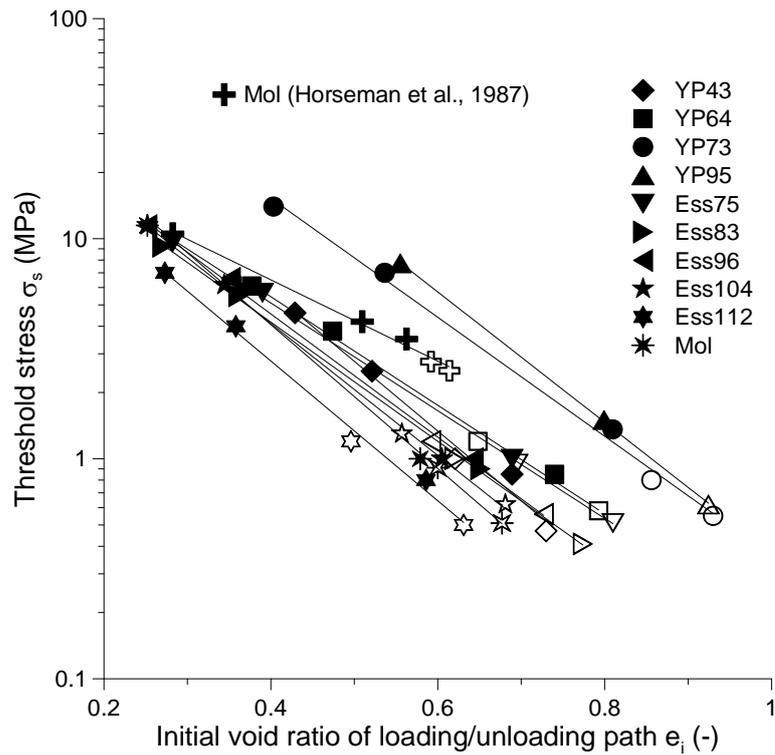


371

372 Figure 2. Swelling stress versus the void ratio just before unloading or reloading for Yprecian  
373 clays - Closed symbols are for unloading path, open symbols for loading path

374

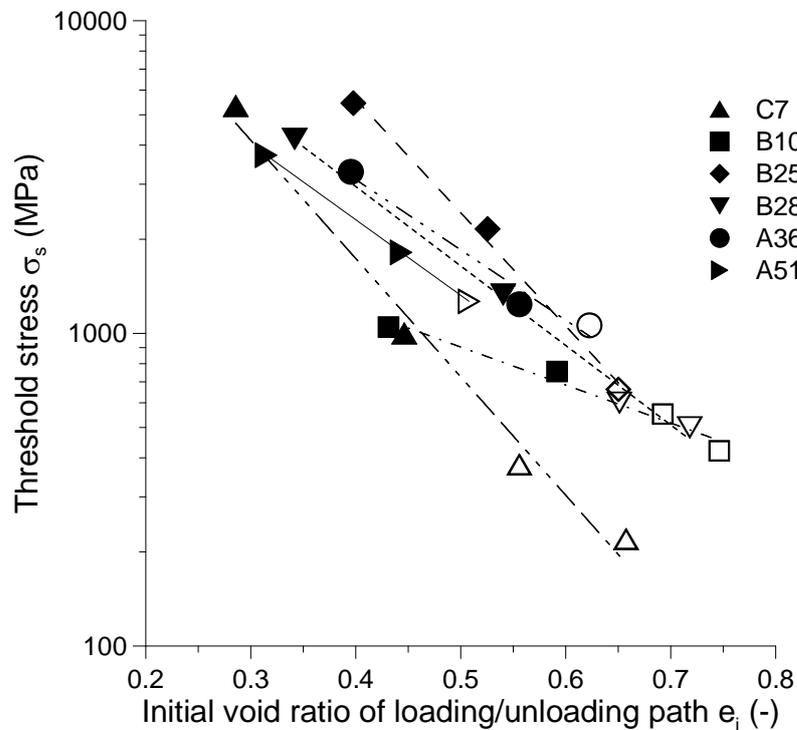
375



376

377 Figure 3. Swelling stress versus the void ratio just before unloading or reloading for Boom  
 378 (from both Essen and Mol sites) and Ypresian clays. - Closed symbols are for unloading path,  
 379 open symbols for loading path

380

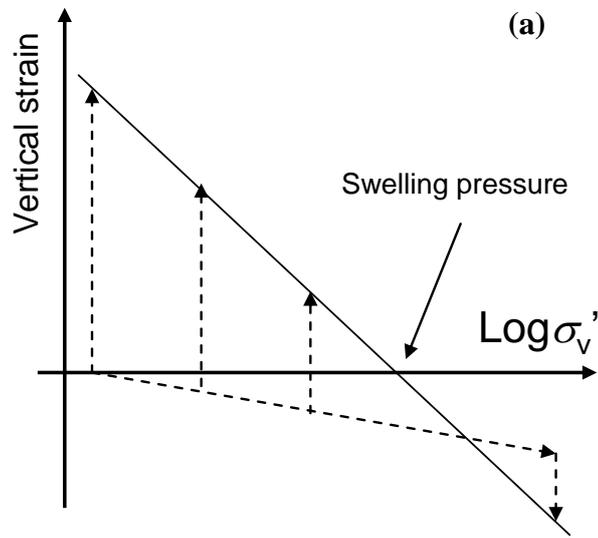


381

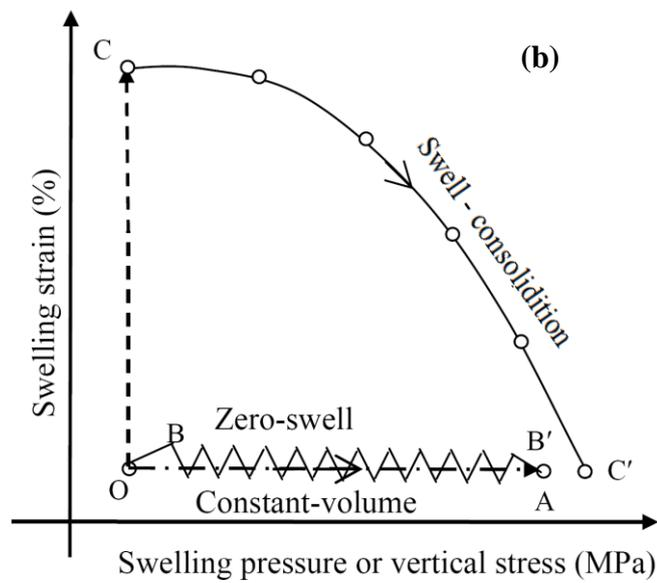
382 Figure 4. Swelling stress versus the void ratio just before unloading or reloading for London  
 383 clay. - Closed symbols are for unloading path, open symbols for loading path

384

385



386



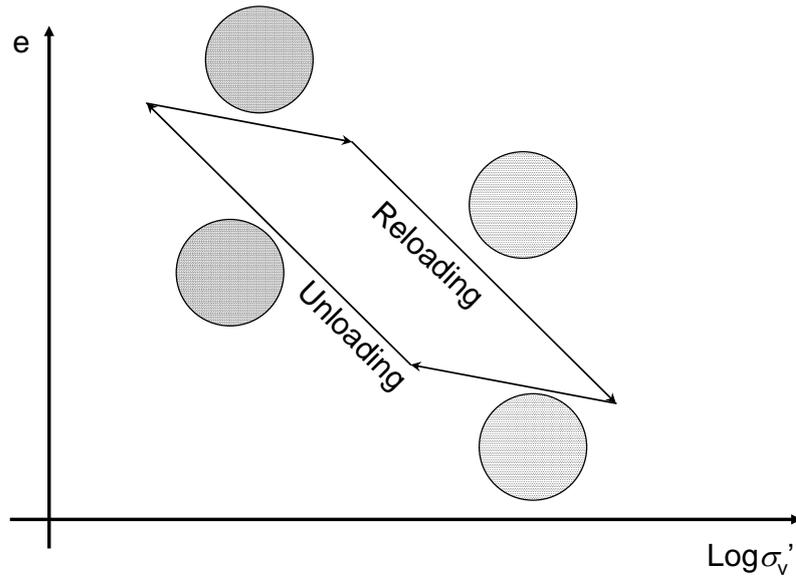
387

388

389

390

Figure 5. Methods for swelling pressure determination. (a) loading-wetting method, (b) constant-volume, zero-swell and swell-consolidation methods



391

392

393

Figure 6. Representation of microstructure changes during unloading/reloading